Quantifying transport between the tropical and mid-latitude lower stratosphere

C. M. Volk*, J. W. Elkins, D. W. Fahey, R. J. Salawitch, G. S. Dutton, J. M. Gilligan, M. H. Proffitt, M. Loewenstein, J. R. Podolske, K. Minschwaner, J. J. Margitan

C. M. Volk, G. S. Dutton, and J. M. Gilligan[1] are with the Cooperative Institute for Research in Environmental Sciences (CIRES) and the Climate Monitoring and Diagnostics Laboratory, National Oceanic and Atmospheric Administration (NOAA), Boulder, CO 80303, U.S.A.
J. W. Elkins is with the NOAA Climate Monitoring and Diagnostics Laboratory, Boulder, CO 80303, U.S.A.
D. W. Fahey is with the NOAA Aeronomy Laboratory, Boulder, CO 80303, U.S.A.
R. J. Salawitch and J. J. Margitan are with the Jet Propulsion Laboratory, California Institute of Technology, Pasadena, CA 91109, U.S.A.
M. H. Proffitt is with the NOAA Aeronomy Laboratory and CIRES, Boulder, CO, 80303, U.S.A.
M. Loewenstein and J. R. Podolske are with the NASA Ames Research Center, Moffett Field, CA 94035, U.S.A.
K. Minschwaner is with the Department of Physics, New Mexico Institute of Mining and Technology, Socorro, NM 87801, U.S.A.

[1]J. M. Gilligan is now with the Department of Physics, Vanderbilt University, Nashville, TN 37235.

*to whom correspondence should be addressed

Submitted to *Science*

Abstract. Airborne in situ observations of CH_4, N_2O, NO_y, O_3, chlorinated halocarbons, and halon-12 11, used in a tropical tracer model, show that mid-latitude air is entrained into the tropical lower stratosphere within -13.5 months; transport is faster in the reverse direction. 13c.cause exchange with the tropics is slower than multi-dimensional models generally assume, ozone at mid-latitudes appears to be more sensitive to elevated levels of industrial chlorine than currently predicted. Nevertheless, approximately 45% of air in the tropical ascent region at 21 km has been entrained from mid-latitudes, implying that emissions from supersonic aircraft could deplete ozone in the middle stratosphere.

Tropospheric air enters the stratosphere predominantly at the tropical tropopause and is then dispersed upward and toward the poles. In the tropics stratospheric air is most efficiently lofted, and photochemistry acts fastest to both produce ozone and convert anthropogenic source gases into reactive compounds that destroy ozone. Exchange of air between the tropics and mid-latitudes is a fundamental component of global stratospheric transport. Because of the profound impact of transport on the distribution of long-lived stratospheric constituents, [heir reactive products, and ozone, models of atmospheric chemistry and transport must accurately represent exchange between tropical and mid-latitude air to provide realistic predictions of perturbations to the ozone layer. 1 'articularl y in t hc lower stratosphere at mid-latitude.s, where observed reductions of ozone exceed mode] predictions (1), concentrations of ozone and related species arc sensitive to transport of air from the tropics (2). Poleward transport from the tropics also dispel scs sulfate aerosols (.?) that provide sites for heterogeneous chemistry, leading to reductions in mid-latitude ozone associated with elevated levels of chlorine (4). Recent work suggests a source for these particles near the tropical t ropopause (5), and major volcanic erupt ions provide a large intermittent source (6). Finally, the rate of mixing of mid-latitude air into the tropics is a key uncertainty in assessing the impact of supersonic aircraft on stratospheric ozone (7).

We present in situ measurements of a suite of trace constituents with photochemical lifetimes spanning more than two orders of magnitude that allow us, in conjunction with a tropical tracer model, to derive rates of mixing into and out of the tropics in the altitude range 16-21 km. Most photochemical models used for prognostic calculations of stratospheric ozone represent transport in two dimensions as rapid meridional mi X i ng superimposed on a zonal-mean circulation with ascent of air in the tropics and descent at mid- and high latitudes (8). Typically, these models extend into the tropics the region where planetary waves break to rapidly mix air (9). In this case, abundances of trace constituents with local photochemical lifetimes longer than -1 year assume common global distributions and arc thus uniquely correlated with each other throughout the stratosphere (*10, 11*). Mixing ratios of some long lived constituents, however, exhibit different relationships in the tropics than at mid- and high latitudes (12, *13*), suggesting the region of rapid

mixing dots not penetrate into the tropics. This conclusion is consistent with satellite observations showing sharp meridional gradients in aerosol and tracer concentrations across the subtropics (6, *14*) and a near] y unattenuated seasonal variation of tropical water vapor (15).

While mixing into the tropics thus seems too slow for efficient global mixing, the question remains how effectively the tropical stratosphere is isolated (*16*). Although model calculations based on meteorological winds have been used to assess transport out of the tropics (17), their ability to infer exchange in the reverse direction appears to be severely limited by the quality of tropical wind data (*18*). Observations of long-lived tracers, however, show some entrainment of mid-latitude air into the tropics (*19*, 20).

Observations. Our measurements were obtained simultaneously from instruments on board the NASA 1:1<-2 aircraft from March through November 1994 (*21*). A new instrument, the Airborne Chromatograph for Atmospheric 'Trace Species (ACATS-IV) measured CFC-11 (CCl_3F), CFC-12 (CCl_2F_2), CFC-113 ($CCl F_2CCl_2F$), CCl_4, $Cl I_3CCl_3$, halon-1211 ($CBrClF_2$), and $Cl I_4$ once every three minutes with instrumental uncertainties generally less than 3% (22). Three other instruments measured N_2O, NO_y (reactive nitrogen), and 0_3 once every second (*23*). We use mid-latitude data from 31 flights obtained at altitudes up to 21 km between 35° and 55° in both hemispheres during fall, winter, and spring. Tropical air was sampled on 4 flights each in late March/early April and in late October. We defined tropical air as the region equatorward of the sharp meridional gradient in the NO_y/O_3 ratio, which delineates the subtropical edge (24).

Tropical tracer model. As an air parcel rises from the tropical tropopause, the mixing ratio of a trace] is governed by production anti loss resulting from both local photochemistry and entrainment of extratropical air. Entrainment is associated with synoptic and planetary scale wave activity on quasi-horizontal isentropic surfaces (2.$). If we assume the net effect of these events at a given altitude is represented by isentropic mixing with air of a mean mid-latitude mixing ratio and that the tropics are horizontally homogeneous, the long-term vertical evolution of a tropical tracer is

given by

$$\frac{\partial \chi}{\partial \theta} Q = P - \frac{\chi}{\tau} - \gamma\chi - \frac{\chi - \chi_{mid}}{\tau_{in}} \qquad (1)$$

where χ ant] χ_{mid} arc the mean tropical and mid-latitude mixing ratios; θ is potential temperature used as vertical coordinate (26); $Q = d\theta/dt$ is the net diabatic hc.sting rate, equivalent to vertical ascent rate (27); P is the photochemical production rate; τ is the life.time for photochemical loss; $\gamma = (\partial\chi/\partial t)/\chi$ is the long-term growth rate; and τ_{in} is a time scale for import of mid-latitude air. The inverse of τ_{in} is the entrainment rate into the tropics, that is the fraction of air in a tropical air volume (at a fixed altitude) imported from mid-] latitudes per unit time interval. in principle, if chemical production, loss, 'growth, and the ascent rate are all known as functions of O, the entrainment time τ_{in} can be determined from observations of tracer mixing ratios in the tropics and mid-latitudes.

We obtained tropical ascent rates, Q, from two independent studies based on radiative transfer calculations and global meteorological and chemical data (28, *29*). O_3 and NO_y have photochemical sources and mall photochemical sinks in the lower tropical stratosphere whereas all other species wc considered have only photochemical sinks, predominantly photolysis in the ultraviolet and reaction with $O(^1D)$ (whereby NO_y is produced from N_2O) or, in the case of CH_4, reaction with 011 and Cl. We calculated diurnall y averaged photolysis rates with a radiative transfer model that includes Rayleigh anti aerosol scattering (*30*). Concentrations of 01 I, $O(^1D)$, Cl, and 1102 (a minor sink for O_3) were calculated with a photochemical model constrained by I R-2 observat ions (*31*). React ion rates and absorption cross sections from the NASA/JPL compendium (32) were used. 1,ong-term growth rates (γ) were derived from observed tropospheric trends during 1993-1994 (*33*).

Vertical profile.s. The degree of isolation of the tropical ascent region can be estimated by compar i son of vertical profiles of tracer mixing ratios observed in the tropics (o profiles calculated

assuming unmixed ascent (unmixed profiles), that is solutions to equation (1) with $\tau_{in}=\infty$ (*34*) (Fig. 1). Observed profiles of the longer-lived species, N_2O and CFC-12, and also of CH_4 and NO_y (not shown) deviate noticeably from unmixed profiles, indicating mixing with photochemically aged mid-latitude air (.3.5), However, for CFC-113 CFC-11, and the shorter-lived species CH_3CCl_3, CCl_4, and halon-1211 (not shown), with lifetimes at 19 km of ~3.1, *2.4,* and 1.1 years, respectively, observed profiles fall within the uncertainty range of values calculated for unmixed ascent.

These results can be understood in terms of the relative influence of photochemistry and isentropic mixing on the evolution of the tracer mixing ratio profiles. For the longest-lived species, photochemistry is so slow that profiles are essentially determined by ascent and mixing. For CFC-11 and other shorter-lived species, photochemical loss occurs rapidly enough to dominate loss by mixing, and hence the vertical profile is controlled primarily by ascent and local photochemistry. Tropical profiles of O_3 can similarly be explained largely by ascent and local photochemical production (occurring on a short time scale of ~3.5 months at 19 km) (*19, 36*) . An estimate of the rate of entrainment of mid-latitude air can readily be obtained from the comparison in Fig. 1: The decline with altitude of the CFC-113 mixing ratio due to chemistry alone (unmixed profile) is comparable to the additional decline induced by mixing (observed profile), implying that chemistry (χ/τ) and mixing ([X-- χ_{mid}]/τ_{in}) are of approximately the same magnitude. Hence, $\tau_{in} \approx \tau (\chi - \chi_{mid})/\chi$, yielding an entrainment time of a few years.

Tracer correlations. Equation (1) can in principle be used to derive τ_{in} (.3'7), but, as shown above, no information about the rate of mixing is contained in observed vertical profiles of species shorter-lived than CIJC-113. Another difficulty in using equation (1) is its dependence on Q that, because of its small value and seasonal and interannual variability, is considered highly uncertain for the tropical lower stratosphere (28, 29). Both deficiencies are avoided by analyzing correlations of tracer mixing ratios. Considering equation (1) for the mixing ratios of two tracers X and Y yields

$$\frac{\partial Y}{\partial X} = \frac{P_y - (\tau_y^{-1} + \gamma_y)Y - \tau_{in}^{-1}(Y - Y_{mid})}{P_x - (\tau_x^{-1} + \gamma_x)X - \tau_{in}^{-1}(X - X_{mid})} \qquad (2)$$

which shows that the functional form of [he. tropical correlation Y(X) dependends only 0 1 1 photochemical production and loss rates, growth rates, the mid-latitude profiles, and the entrainment time. Furthermore, correlation diagrams eliminate much of the scatter attributed to atmospheric fluctuations because spatial and temporal variations for lcmg-lived stratospheric tracers arc correlated (*38*). Therefore, correlations provide a more reliable measure of atmospheric transport than vertical mixing ratio profiles.

Differences in the slopes of correlat ions observed at mid-lat it udes and in the tropics provide a direct measure of exchange between the two regions. If isentropic mixing is fast compared to photochemistry for two tracers throughout the mid-latitudes and the tropics, one tight correlation will exist for all latitudes, with a shape determined by the global photochemical sources and sinks of both species (*11*). If mixing into the tropics is slow compared to photochemistry for both species, the tropical mixing ratios will be influenced solely by local (tropical) photochemical sources and sinks. Two species with sufficiently different spatial distributions of sources and sinks wiil then exhibit a correlation in the tropics with a slope different from that at mid-latitudes (*16*). Finally, if mixing is slow compared to photochemistry for only one of the two species, the difference of the correlat ion slope in the tropics from the slope at mid-lat it udes wi ll be sensit ive to the magnitude of mixing into the tropics.

For a given mixing ratio of N_2O, the shorter-lived species show lower abundances in the tropics than at mid-latitudes because their loss processes arc significant near ~20 km whereas N_2O is not destroyed until the air reaches higher altitudes (prior to dc.scent back to low altitude, mid-latitude regions) (Fig. 2). Because the abundance of N_2O in the. tropics is sensitive to isentropic mixing, however, the tropical correlations do not match the correlations calculated assuming unmixed ascent (unmixed correlations). The separation of tropical and mid-latitude correlations is most pronounced for haicm-121 1 (the shortest-lived tracer) and diminishes for species with increasing photochemical lifetime, as local chemistry becomes less important relative to mixing in

determining the tropical abundance of each tracer. Tropical correlations of the longer-lived species ([;]'C-113, CFC-12, CH_4, and NO,) with N_2O (not shown) exhibit the same slope as lnici-latitude correlat ions, imp] ying that over the altit ude range sampled by the ER-2 the local photochemical time scales of these compounds arc long compared to mixing time scales. Quantification of mixing rates using these longer-lived species requires correlations with a molecule whose evolution is dominated by local photochemistry, such as O_3 (1 'ig. 3). in such a comparison, the slope of the tropics] correlation is most sensitive to mixing for the longest-lived species. Tropical correlations of the shorter-lived species (CFC- 11, CH_3CCl_3, CCl_4, and halon-121 1) with O_3(not shown) are similar to the unmixed correlations ant] thus do not provide quantitative information about mixing.

Rates of transport. The correlation diagrams in Figures 2 and 3 can bc used to dc.rive rates of transport between the tropics and mid-latitudes during the measurement period. Wc integrate equation (2), constrained by mixing ratios for nlid-latitudes from our observations and computed photochemical sources and sinks (.?0, *31*), to calculate the tropical correlation Y(X) of two species, treating the entrainment time τ_{in} as a free parameter (.?9). Direct inversion of equation (2) to yield a value of τ_{in} as a function of altitude is not practical because the tropical tracer measurements exhibit too much variability to define the slope of the correlation diagram at each altitude (40). Initially, wc assume a value for τ_{in} independent of altitude. For each pair of tracers displayed in Figures 2 and 3, wc determined the value of τ_{in} giving best agreement with the observations by an iterative least-squares fit of the calculated correlation (shown in Fig. 2 and 3) to the observed tropical correlation. Analysis of each correlation diagram (Fig. 4) yields a geometric mean (weighted by the individual uncertainties) for τ_{in} of] 3.5 months, with an uncertainty of -20% (d]). Individual determi nat ions of τ_{in} from each pair of [racers agree with this mean value. This result is indicative of a seasonall y and vertical i y averaged entrainment rate into the tropics of 7% per month (1/Tin) over the altitude range 16-21 km during 1994. The average entrainment time of 13.5 months is longer than the time scale for isentropic mixing at mid-latitudes of less than 3 months (42), confirming that mixing into the tropics is slow compared to mixing within mid-latitudes.

The data do not provide information on the dependence of τ_{in} with height. Following the inversion procedure outlined above, but allowing τ_{in} to vary linearly with altitude, we found no evidence for either a significant increase or decrease of the entrainment time with altitude. This result is also evident by the good fits to the observed correlations using values of τ_{in} independent of altitude (Fig. 2 and 3). Conceptually, the altitude dependence of τ_{in} is implicit in the detailed shape of the tropical correlation. The tropical correlations displayed in Figures 2 and 3, because of their variability and limited range, do not reveal details about their shape much beyond their average slope, and thus they do not allow a good estimate of the altitude dependence of τ_{in}. Another complication is posed by the convolution of space and time not implicit in the time-averaged formulation of Eq. (1): Because tropical air at any given altitude carries the integrated signature of mid-latitude intrusions from the time it crossed the tropopause, the detailed shape of the tropical correlation at a given time is determined not solely by the altitude dependence of isentropic mixing, but also by the time history of mixing, photochemistry, and mid-latitude abundances. Consequently, tropical and mid-latitude measurements from many different seasons are needed to unravel the temporal and height dependence of τ_{in}; neither can be determined from our tropical observations covering only two seasons. However, a seasonal average is implicit in our vertically averaged determination of τ_{in} since the observations cover an altitude interval that a rising air parcel crosses during the course of several seasons (4.?).

Equatorward entrainment of air into the tropics is not necessarily balanced by poleward detrainment from the tropics. A rough estimate for the rate of detrainment can be made assuming a steady mass balance across the subtropical edge and the rate of entrainment determined above. In the annual mean, the net mass flux out of the tropics (detrainment minus entrainment) must be balanced by the mean mass divergence within the tropics (determined from the mean ascent rate):

$$\frac{\rho}{\tau_{out}} - \frac{\rho}{\tau_{in}} = -\frac{\partial}{\partial z}(\rho w) \qquad (3)$$

where τ_{out} is a time scale for export of air; ρ is the air density; z is altitude; and w is the mean

vertical velocity. The inverse of τ_{out} is the mean detrainment rate, that is the fraction of air in a tropical air volume (at a fixed altitude) exported to mid-latitudes per unit time. Detrainment rates compute.ci from equation (3) for our estimate for τ_{in} (13.5 months) and ascent velocities averaged over *24 months (28, 29) show* that, over much of the altitude range considered, more air is exported from the tropics than is imported (Fig. 5A). The derived detrainment rates and their vertical profiles arc dominated by the mass divergence term and arc not very sensitive to τ_{in} (44). These rates should be indicative of the total transport from the tropics to both hemispheres in a 2-ycar average. The corresponding detrainment time (τ_{out}) of less than ~6 months below 19 km is consistent with observations of rapid propagation of the seasonal cycles of CO_2 and H_2O from the tropics to mid-latitudes in the lowest several kilometers of the stratosphere (42, *45*). These observations also show a fading of the seasonal signals of CO_2 and H_2O at mid-latitudes above 19 km, indicating slower detrainment from the. tropics at these altitudes. This morphology of dc.creasing detrainment at higher altitudes is also supported by studies of aerosol dispersal from the tropical reservoir (*3*, 6) and by transport analyses based on meteorological winds (*17*, *18*). Recent analysis (*18*) has shown that transport rates from the tropics to the northern hemisphere are about 8 to 10% (of tropical mass) per month at 18.5 and 21 km, in reasonable agreement with our result of a total detrainment rate to both hemispheres of 5 to 35% in this altitude range.

As shown in Fig. 5B, approximately 45% of air of extratropical origin accumulates in a tropical air parcel during its ~8 month ascent from the tropopause (o 21 km. This estimate assumes an entrainment lime of 13.5 months and that newly entrained air is rapidly homogenized in the tropics. The result is insensitive to the altitude dependence of the entrainment rate, but depends directly on the magnitude of the ascent velocity and thus has a large uncertainty (Fig. 5B). Regardless, entrainment of mitt-latiludc air into the tropical ascent region of the lower stratosphere is significant.

implications. Our measurements and analysis demonstrate that tropical air is relatively isolated from mid-latitudes, where isentropic mixing occurs more rapidly. However, because the time

scale for tropical ascent is comparable to the entrainment time scale, there is considerable accumulation of extratropical air in the inner tropics. Our observations suggest that nearly half the air in t he tropical ascent region at 21 km has been transported from mid-lat it udes. 'I 'his implies that a significant fraction of NO_x (= NO+NO_2) and other effluents emitted from supersonic aircraft at mid-latitudes between 16 and 23 km will likely reach the middle and upper stratosphere, where enhancements in NO_x arc expected 10 lead to reductions ill ozone (7). While estimating the effects of human activity on ozone remains a task for multi-dimensional models of atmospheric transport and chemistry, our determination of the rates of transport and the fraction of mid- latitude air within the tropical ascent region const itutes important tests for t he accuracy of such models. Current 1 y, most models overestimate the magnitude of exchange between the tropics and mid-latitudes (6'). Restricting exchange with the tropical production regions of Wont would enhance the relative in fluence of chemical sinks on ozone concentrations at mid-latitudes. Mid-latitude ozone should thus be more sensitive to enhanced chemical loss induced by elevated levels of industrial halocarbons and volcanic aerosols, than current models predict. Tests with a two-dimensional model indicate that calculated ancl observed reductions of ozone at mid-latitudes agree better if transport parameters arc modified to simulate restricted exchange across the tropics (46). A more realistic representation of dynamical coupling between the tropical source, and mid-latitude sink regions of ozone may thus hold the key to understanding and reliabl y predicting the response of the stratospheric ozone 1 ayer (o a variet y of anthropogenic as wel i as natural pert urbations.

References and Notes

1. Global Ozone Research and Monitoring Project - Rep. 37 (World Meteorological Organization, Geneva, 1995).

7. M. K. W. Ko, N. D. Sze, D. K. Weisenstein, *J. Geophys. Res.* 94, 9889 (1 989).

3. C. R. Trepte, R. E. Veiga, M. P. McCormick, *ibid.* 98, 18563 (1993).

4. G. Brasseur and C. Granier, *Science* 25’7, 1239 (1 992); D. W. Fahey *et* al., *Nature* **363**, S09 (1993); J. C. Wilson *et al.*, *Science* **261**, 1140 (1993).

5. C. A. Brock, P. Hamill, J. C. Wilson, H. H. Jonsson, K. R. Chan, *Science* 270, 1650 (1995).

6. C. R. Trepte and M. J. Hitchman, *Nature* **355**, 626 (1 992); M. H. Hitchman, M. McKay, C. R. Trepte, *J. Geophys. Res.* 99, 20689 (1994).

7. R. S. Stolarski *et al.*, *NASA Ref. Publ. 1391* (1995).

8. M. J. Prather and E. E. Remsberg, Eds., *NASA Ref. Publ. 1292* (1993).

9. M. E. McIntyre and T. N. Palmer, *Nature* **305**, 593 (1983).

10. J. R. Holton, *J. Geophys. Res.* 91, 2681 (1986); J. D. Mahlman, H. Levy 11, W. J. Moxim, *ibid.*, 2687.

11. R. A. Plumb and M. K. W. Ko, *ibid. 97,* 10145 *(1992).*

12. P. D. Goldan, W. C. Kuster, D. L. Albritton, A. L. Schmeltekopf, *ibid.* 85, 413 (1 980); M. 11. Proffitt, D. W. Fahey, K. K. Kelly, A. F. Tuck, *Nature* **342**, 233 (1989).

13. D. M. Murphy *et* al., *J. Geophys. Res.* 9 S, 8751 (1993); f ahey *et al.*, manuscript submitted to *Geophys. Res. Lett.*

14. W. J. Randel *et al.*, *Nature* **365**, 533 (1993).

15. P. W. Mote *et al.*, *J. Geophys.Res.* **1 01, 3989 (] 996).**

16. **R.** A. Plumb, *ibid.,* 3957.

17. R. Rood, A. Douglass, C. Weaver, *Geophys. Res.Lett.* 19, 805 (1992); 1'. Chen, J. R. Holton, A. O'Neill, R. Swinbank, *J. Atmos. Sci. S1, 3006 (1* **994).**

18. D. W. Waugh, *J. Geophys. Res.*, 101, **4007 (1 996).**

19. L. M. Avallone and M. J. l'rather, *ibid.,* 1457.

20. K. Minschwaner *et al., ibid,, in press.*

21. During the flight campaign, the Airborne Southern Hemisphere Ozone 1 Experiment/ Measurements for Assessing the Effects of Stratospheric Aircraft (ASHOE/MAESA), the ER-2 sampled air from 60° N to 70° S up to ? 1 km.

22. J. W. Elkins *et* al., *Geophys. Res. Lett.*, 23, 347 (1996).

23. J. R. Podolske and M. Loewenstein, *Appl. Opt. 32, S324 (1993);* D. W. Fahey *et* al., *J. Geophys. Res.*, 94, 11299 (19'89); M. 11. Proffitt and J. Mc] aughlin, *Rev. Sci. Instrum.* S4, 1719 (1983). Data used here are averaged over 10 second intervals.

24. As shown in (13), the NO_y/O_3 ratio is markedly lower in the tropics than anywhere else in the stratosphere. Hence, NO_y/O_3 is a good tracer for tropical air. The latitudinal range of the selected tropical data varied from flight to flight and between the two seasons sampled. The tropical observations span 10° *N* to 26° *S* in late March/early April 1994 and 19° N to 14° S in late October 1994; most of the data fall within 12° of the equator.

25 In the following, "exchange" bet wccn the tropics and mid-latitudes and related terms will refer to isentropic, that is adiabatic, processes.

26. Potential temperature is the temperature an air parcel would attain if it were adiabatically compressed or *expanded* from the local pressure to 10$ Pa. Potential temperature is a

conserved quantity for isentropic, air motions and is a monotonically increasing function of altitude in the stratosphere. Its use as vertical coordinate in equation (1) is convenient because isentropic mixing occurs horizontally in this coordinate system.

27. If potential temperature θ is used as vertical coordinate, a vertical displacement implies diabatic gain or loss of heat.

28. K. 1 I. Rosenlof, *J. Geophys. Res.* **100**, 5173 (1995). We averaged from 10° N to 00 S and over a 24-month period (September 1992 to August 1994). The uncertainty of these calculations in the lower stratosphere is estimated as -50% above 18 km and even more just above, the tropopause.

29. J. Eluszkiewicz *et al., J. Atmos. Sci.* **53**, 217, 1996. We averaged as described above (28). Uncertainties are estimated as -50%. The averaged tropical heating rates agree with those obtained from *(28)* within the estimated uncertainties.

30. K. Minschwaner, R. J. Salawitch, M. B. McElroy, *ibid. 98,* 10543 *(1993).* The model is constrained by vertical profiles for O_3 from a climatology scaled to match total column measurements from TOMS, and vertical profiles for temperature and aerosol extinction from the National Meteorological Center and the Stratospheric Aerosol and Gas Experiment 11, respectively. We averaged photolysis rates calculated for winter, summer, and equinox, and for latitudes from 10° N to 10° S. Uncertainties in the photolysis rates are -20% for most species.

31. R. J. Salawitch et *al., Geophys. Res. Lett.* **21**, 2251 (1994).

32. *Chemical Kinetics and Photochemical Data for Use in Stratospheric Modeling, Evaluation No. 11, JPL Publ.* 94-26 (NASA, Jet Propulsion Laboratory, Pasadena, CA, 1994).

33. S. A. Montzka *et al., Science,* in press; J. W. Elkins, E. J. Dlugokencky, unpublished data from the NOAA/CMDL global network. Methods and trend analysis are described in: J.

W Elkins *et al., Nature 364, 780* (1 993); E. J. Dlugokencky, L. P. Steele, P. M. Lang, K. A. Masarie, *J. Geophys. Res.*, 99, 17021 (1994). Only data from tropical stations was used. Although the growth rates are smaller than a few %/year, they are generally of the same order as photochemical loss rates near the tropical tropopause.

34. The unmixed case corresponds to the "tropical pipe" model in *(16).*

35. Mid-latitude air in the lower stratosphere has in general at one time been lofted to higher altitudes in the tropics, before descending in the downward branch of the stratospheric circulation cell. Because of the increasing intensity of ultraviolet radiation with altitude, (his air has "photochemically aged", resulting in lower mixing ratios for the species displayed in Fig. 1 at mid-latitudes than in the tropics.

3(). A. 1;. Dessler *et* al., .1. *Atmos. Chem.*, in *press.*

37. This approach is pursued in (20).

38. D. H. Ehhalt, E. P. Röth, U. Schmidt, *J. Atmos. Chem.*, *1,* 27 (1983).

39, 1 'or the integration, all observational inputs are first established as functions of potential temperature θ. Mean mid-latitude mixing ratios for N_2O, O_3, and NO_y (the species sampled at high frequency) are obtained from non-parametric "1ocss" fits *(48)* versus O. I 'or the other species (where much less data is available) mean mid-latitude mixing ratios are then deduced from quadratic fits to the mid-latitude correlations versus N_2O or O_3 as shown in Figures 2 and 3. A relationship between O and the tropical mixing ratios X (of N_2O and O_3), again from a 1ocss fit versus *O,* is then used to transform the coordinate system from **0** to **X ,** Finally, Equation (2.) is solved as differential equation of Y in X to calculate the tropical correlation, Y(X). **in** itial (tropical tropopause) mixing ratios are obtained by averaging **all** measurements taken in the upper tropical troposphere during the flight campaign.

40. The shape of τ_{in} as function of altitude determined by direct inversion of equation (2) depends sensitively on the choice of functional fit to the data to determine dY/dX versus altitude; its geophysical meaning is therefore questionable.

41. Because uncertainties for individual determinations of τ_{in} as provided by sensitivity tests were approximatel y symmetric on a logarithmic rather than a 1 inear scale, wc evaluated all statistical quantities for $\log(\tau_{in})$ rather th an τ_{in}. The weighted mean is thus equivalent to a weight ed geometric mean and its uncertaint y is best expressed as an uncertai nt y factor that evaluated to 1.2.

42. K. A. Boering *et al.*, *Geophys. Res. Lett. 21, 2567 (1994);* B. J. Hintsa *et al.*, *ibid.*, 2.559; K. A. Boering *et al.*, *Geophys. Res.* 1.('//.22,2737(1995).

43. Based on the ascent rates from (*28, 29*), ascent of tropical air from the tropopause to 21 km takes ~8 months, Hence, the two observational snapshots in March/April anti October 1994 combine air influenced by mixing during the time span of at least a full seasonal cycle. Differences between the March/April and October observations on a given potential temperature level were generally smaller than flight-to-flight variability.

44. Because of the large uncertainty in the ascent rates (26', 29), mean detrainment rates obtained by this simple argument must be considered uncertain to at least 50%. The increase above 19 km in the detrainment rate based on (29) is an artifact caused by a known low bias in MI SO_3 satellite Immurements at 46 hPa (29).

45. M. 1'. McCormick *et al.*, *J. Geophys. Res.* **98**, 4867 *(1993).*

46. M. K. W. Ko, private communication. The model calculated the decadal ozone change. *between 1980* and 1990 as well as the transient ozone change in response to increased aerosol loading after the eruption of Mt. Pinatubo in June 1991. A description of the model is given in: M. K. W. Ko, K. K. Tung, D. K. Weisenstein, N. D. Sze, *J. Geophys. Res.*,

90, 2313 (1985); the modifications in model transport are briefly described in: D. K. Weisenstein, M. K. W. Ko, N. D. Sze, J. M. Rodriguez, *Geophys. Res. Lett. 23, 161* (1996).

47. The effective lifetime is T = 1/(7' [+ 'y). '1' is the relevant lime scale for the combined effects of local growth and photochemical loss that determine the vertical profile of the tropical abundance in the absence of mixing. Because photochemical 10ss is the dominant factor (above -18 km) for the spc.tics considered here, we refer to '1' simply as lifetime or photochemical lifetime.

48. W. S. Cleveland, *J. Amer. Stat. Assoc.* 74, 829 (1979).

49. Wc thank K. II. Rosenlof and J. Eluszkiewicz for providing data for tropical ascent rates and suggestions and K. R. Chan for mc[c.orological data measured from the ER-2 aircraft. Support during the field deployments in New Zealand by P. J. Fraser, L. P. Steele, M. 1'. Lucarelli, and S. A. Montzka is appreciated. We have also benefited from discussions with R. A. Plumb and F. L. Moore. We finally thank our many colleagues of the 1994 ASHOE/MAESA campaign, especially the pilots of the ER-2 aircraft. This rc.search is supported in part by NASA's Upper Atmospheric Research Program and the At mospheric Effects of Stratospheric Aircraft component of the NASA High-Speed Research Program. A portion of this research was carried out by the Jet Propulsion 1.aboratory, California Institute of Technology, under a contract with the National Aeronautics and Space Administration.

Figure captions

Fig. 1. Vertical profiles of mixing ratios of several long-lived trace species in the tropics (gray dots) and mid-latitudes (black squares with error bars). For the mid-latitudes, the data was binned into 10K increments of potential temperature (0); the profiles shown represent the bin averages and the error bars represent the standard deviation within each bin. Solid lines are calculated tropical profiles for unmixed ascent ($\tau_{in}=\infty$) from 0=380K (the approximate mean tropopause height for the tropical observations). Calculated profiles are shown for ascent rates Q from (*28*); profiles based on ascent rates from (*29*) are similar to the ones shown. Dashed lines represent an uncertainty range. inthccalculatcci imiilcsjn(iucc(ihy a SO% uncertainty in Q. Also indicated is the effective lifetime '1' *(47)* at 0=440 K (-19 km altitude) for each of the species. Species (not shown) that are shorter-lived than CFC-11 behave similarly to CFC-11, that is their tropical profiles agree with the unmixed profiles, within the limits of uncertainty. In particular, the observed O_3 profile is closely matched by the calculated unmixed O_3 pmfile.

Fig. 2. Correlations of mixing ratios for tile simrtcr-lived species versus N_20 in the tropics (dark gray dots) anti at mi(i-latitudes (light gray dots). Thin solid lines represent mean mid-latitude correlations used in the model and were obtained from quadratic fits to the correlations. 1 Dashed lines are calculated cor relations for the unmixed case ($\tau_{in}=\infty$). Thick solid lines are calculated tropical correlations for a constant entrainment time τ_{in} that yielded the best agreement (in a least-squares sense) with the observed tropical correlations. Ail fits are shown over a N_2O range that corresponds to the potential temperature range. 0=380K to 0=493K (the stratospheric O-range of

the tropical data). Also indicated is the effective lifetime T (*47*) at θ=440 K for each of the species.

Fig. 3. Correlations of mixing ratios for the longer-lived species versus O_3. Colors and lines have identical meaning as in 1 ig. **2.** For N_2O and NO_y, mean mid-latitude correlations (thin solid lines) are from non-parametric "loess" fits (*48*) of each species versus O. For all other species, they are quadratic fits to the mid-latitude correlations. Effective lifetimes T (*47*) at θ=440 K ate indicated for the species with photochemical sinks.

Fig. 4. Entrainment times Tin obtained from each of the correlations shown in Figures 2 anti 3 as the constant that yielded the best agreement (in a least-squares sense) of the calculated to the observed tropical correlat ions. Error bars were obtained from a series of sensitivity tests to uncertainties of all the inputs used in the calculation (including uncertainties of fits and initial values) under the assumption that individual inputs are independent of each other. The error bars are symmetric on a logarithmic scale (*41*). The solid black line is the weighted geometric mean (1 3.5 months); its uncertainty (not shown), expressed as uncertainty factor, is 1.2. Dashed lines reflect the range of one standard deviation.

Fig. 5. (A) Entrainment rate into and detrainment rates out of the tropics versus altitude, expressed as % of air within a tropical air volume (at a fixed altitude) entrained/detrained per month. Results are for τ_{in}=13.5 months and ascent rates from (*28*) (dashed line) and *(29)* (dotted line). The disagreement bet ween detrainment rates based on (28) and (29) reflects differences in the vertical profiles of the ascent rates (*44*). (B) Fraction of mid-latitude air within the tropics versus altitude for nominal (solid line) and extreme (dashed lines) values of τ_{in} and ascent rates w from (28) as indicated. The corresponding result for ascent rates from (29) agrees to within -5%. To facilitate comparison with Fig. 1, the approxi male potential temperature (valid for both A and

B) is given on the right axis.

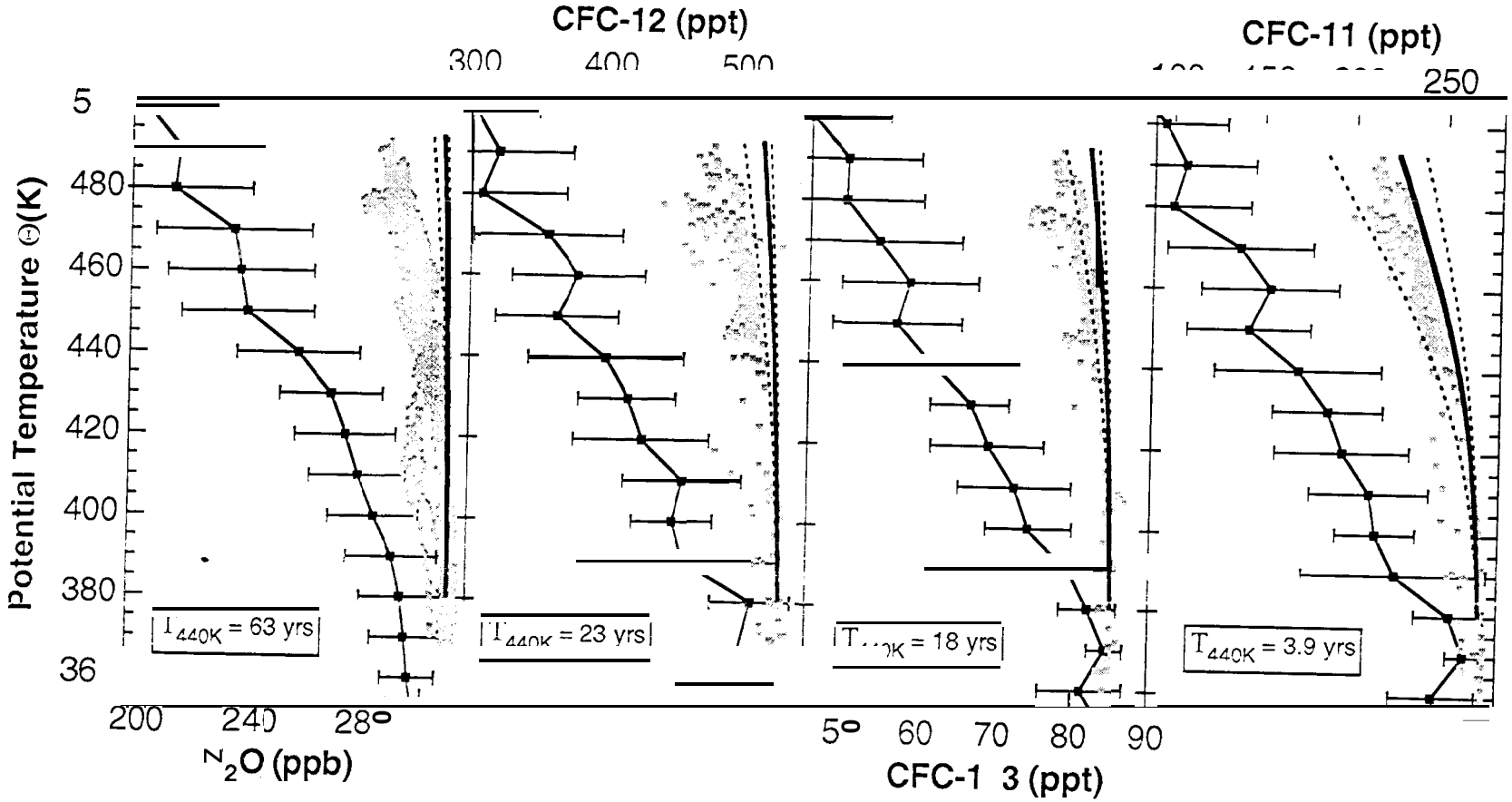
CFC-12 (ppt)
300
400
500
CFC-11 (ppt)
250
Potential Temperature Θ(K)
5
480
460
440
420
400
380
36
T_{440K} = 63 yrs
T_{440K} = 23 yrs
T_{440K} = 18 yrs
T_{440K} = 3.9 yrs
200
240
28°
N_2O (ppb)
5°
60
70
80
90
CFC-1 3 (ppt)

Figure 1

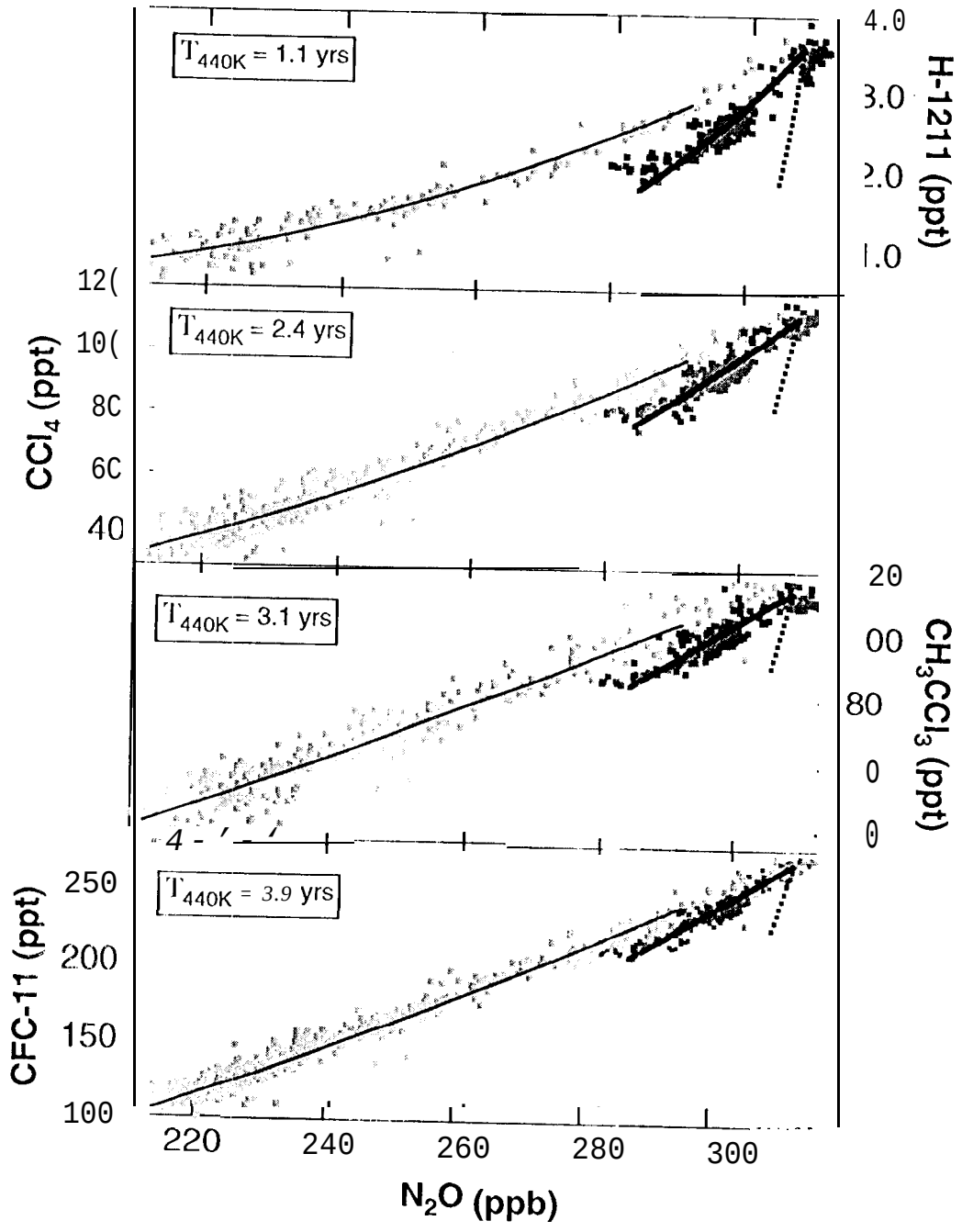
T_{440K} = 1.1 yrs
T_{440K} = 2.4 yrs
T_{440K} = 3.1 yrs
T_{440K} = 3.9 yrs
H-1211 (ppt)
4.0
3.0
2.0
1.0
CCl_4 (ppt)
12(
10(
8C
6C
40
CH_3CCl_3 (ppt)
20
00
80
0
0
CFC-11 (ppt)
250
200
150
100
220
240
260
280
300
N_2O (ppb)

Figure 2.

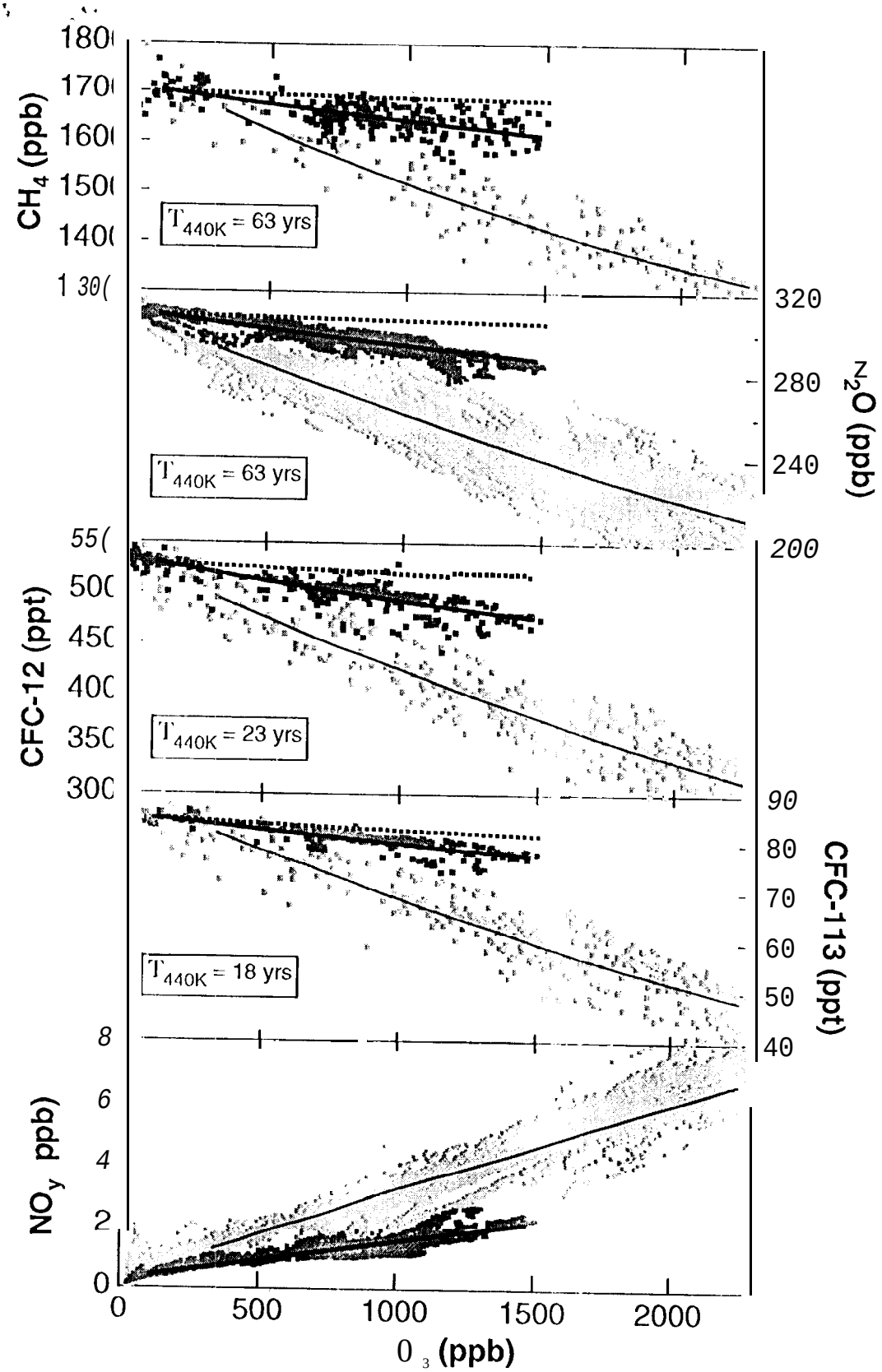
CH4 (ppb)
T440K = 63 yrs
N2O (ppb)
T440K = 63 yrs
CFC-12 (ppt)
T440K = 23 yrs
CFC-113 (ppt)
T440K = 18 yrs
NOy ppb)
0 500 1000 1500 2000
0 3 (ppb)

Figure 3.

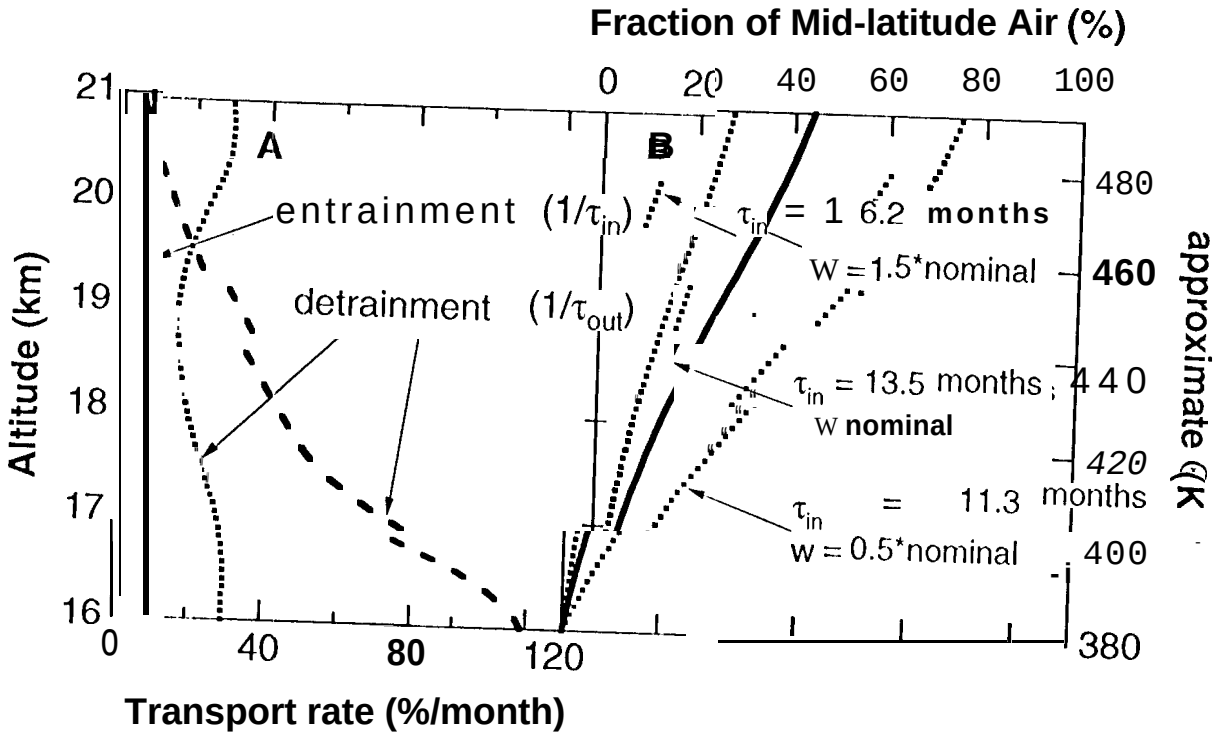
Fraction of Mid-latitude Air (%)
0
20
40
60
80
100
21
20
19
18
17
16
A
B
entrainment (1/τin)
detrainment (1/τout)
τin = 16.2 months
w = 1.5*nominal
τin = 13.5 months
w nominal
τin = 11.3 months
w = 0.5*nominal
480
460
440
420
400
380
Altitude (km)
approximate θK
0
40
80
120
Transport rate (%/month)

Figure 5.